Electronic Supplementary Material (ESI) for Materials Chemistry Frontiers.

Supporting Information

Nanoconfining Red Phosphorus within MOF-derived Hierarchically Porous Carbon Networks for High Performance Potassium Storage

Jinqian Cheng, Zibin Liang, Yingxiao Wu, Degao Wang, Tianjie Qiu, Yanqun Tang, Jinming Shi, Dingguo Xia and Ruqiang Zou*

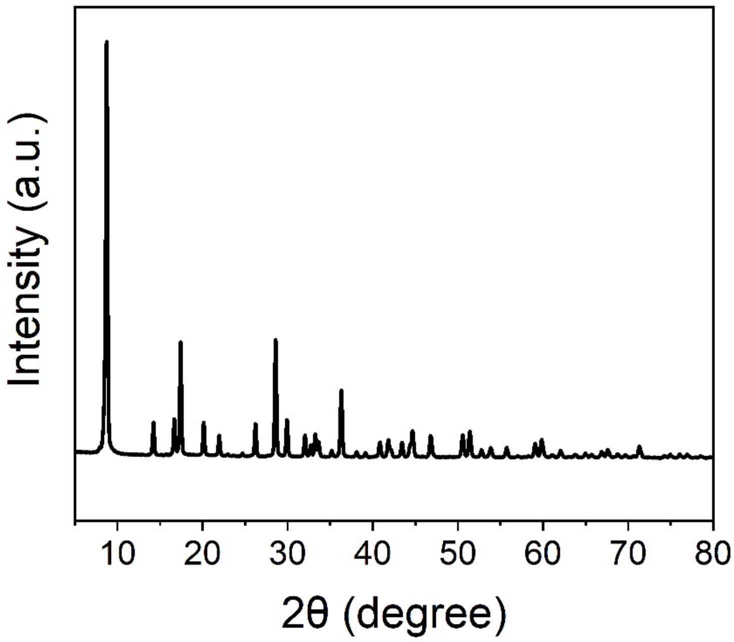

Figure S1. XRD pattern of MET-6.

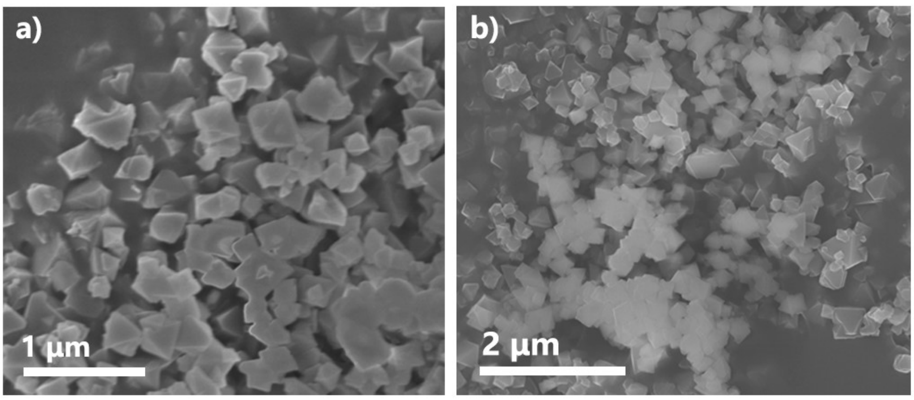

Figure S2. SEM images of MET-6.

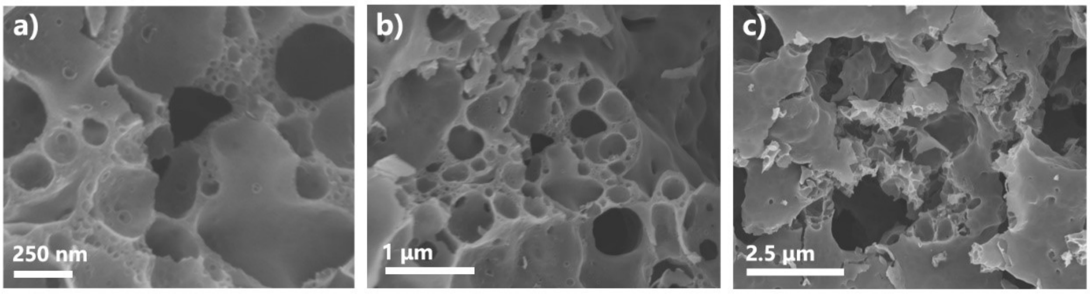

Figure S3. SEM images of CN.

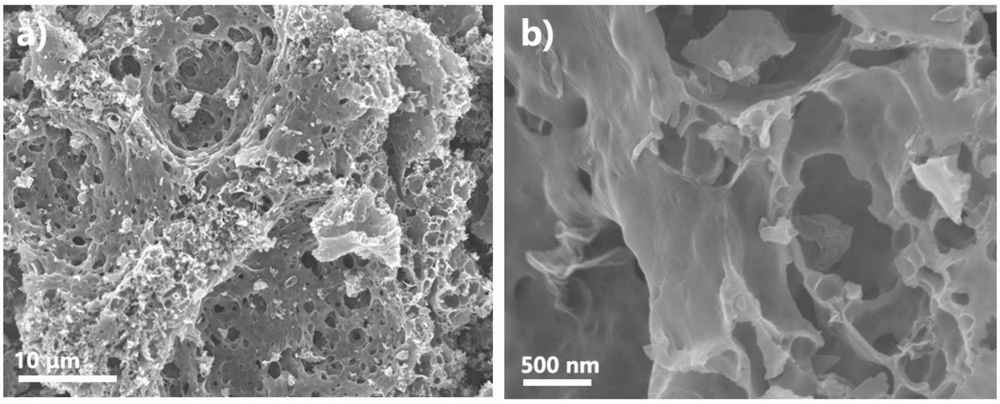

Figure S4 SEM images of HPCN.

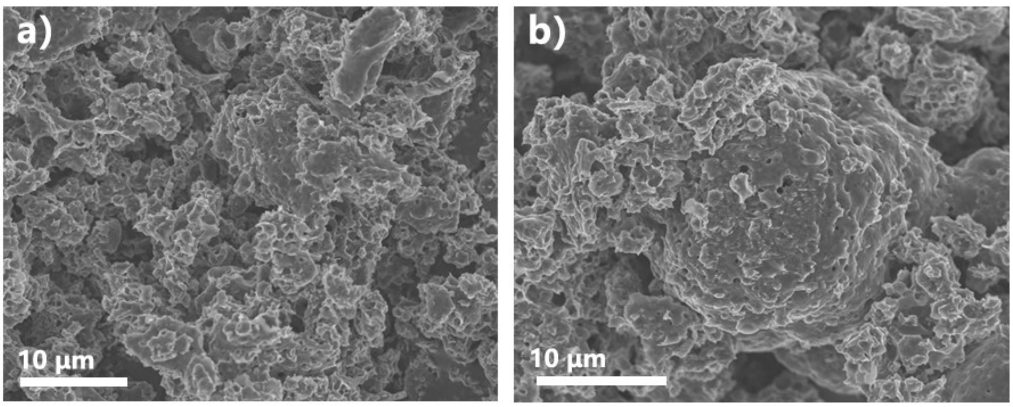

Figure S5 SEM images of P@CN.

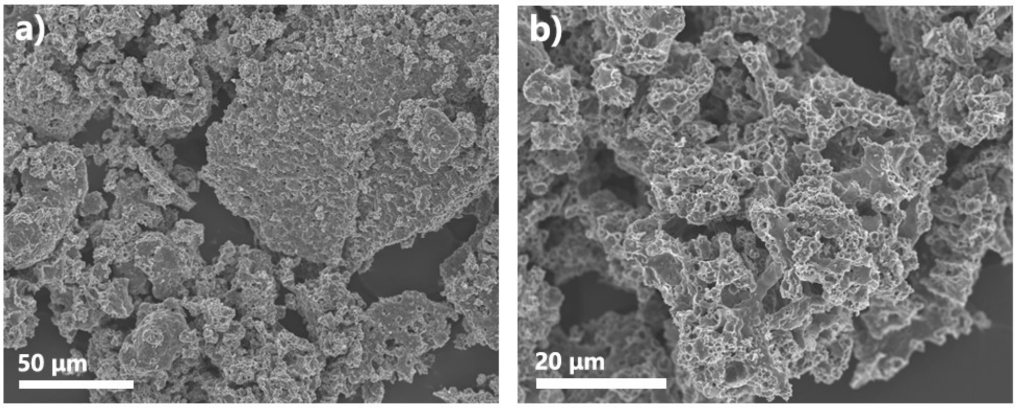

Figure S6 SEM images of P@HPCN.

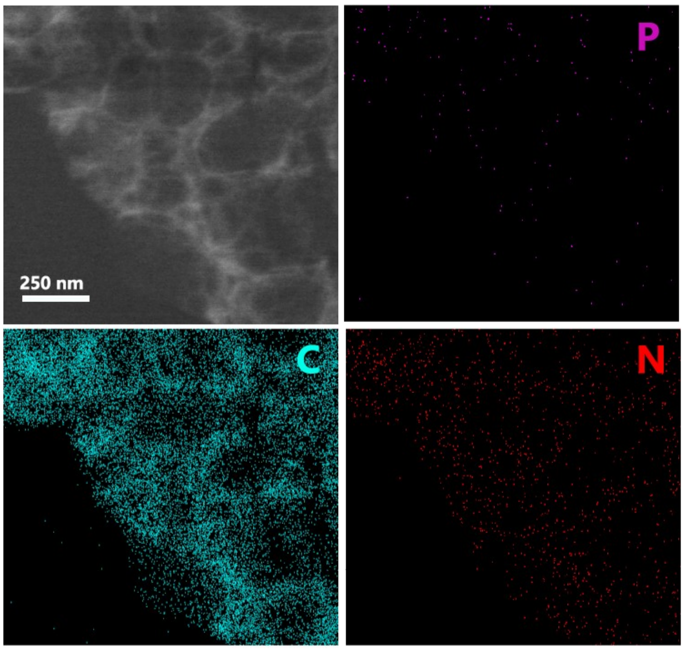

Figure S7 HAADF-STEM images and corresponding EDS profiles of HPCN.

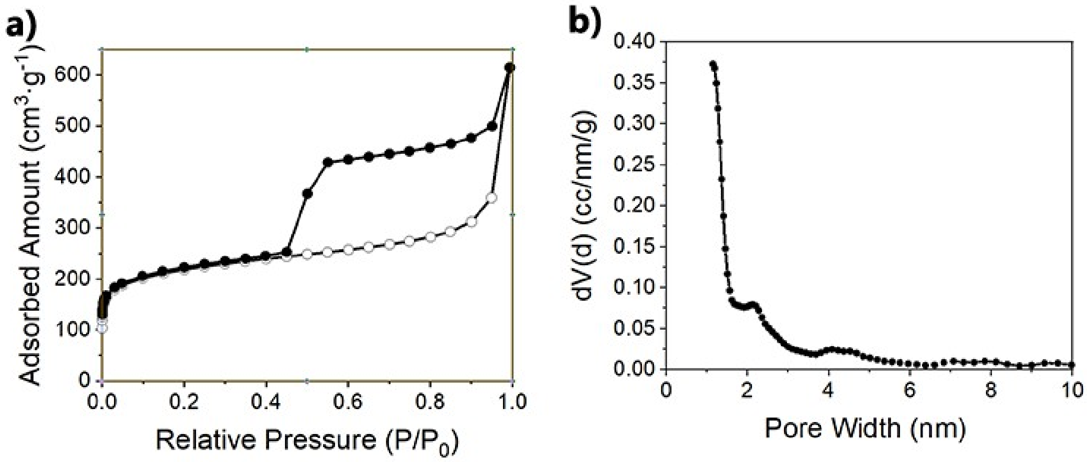

Figure S8. (a) Nitrogen sorption isotherm and (b) corresponding pore size distribution of CN.

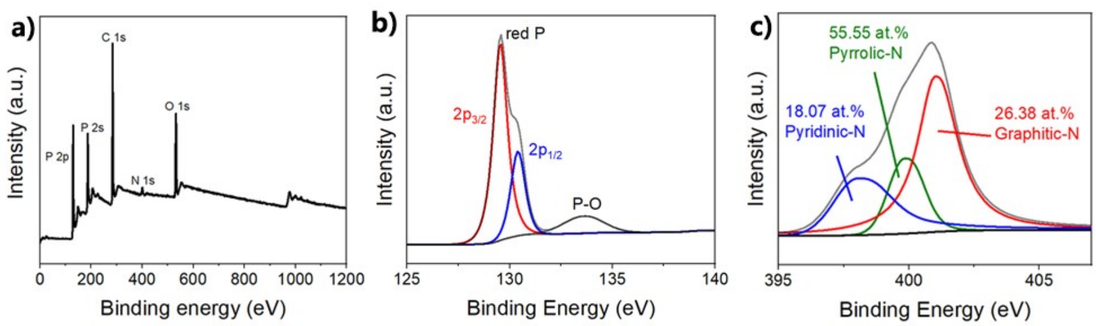

Figure S9. (a) Full XPS spectrum, (b) high-resolution P 2p spectrum, and (c) high-resolution N 1s spectrum of P@CN.

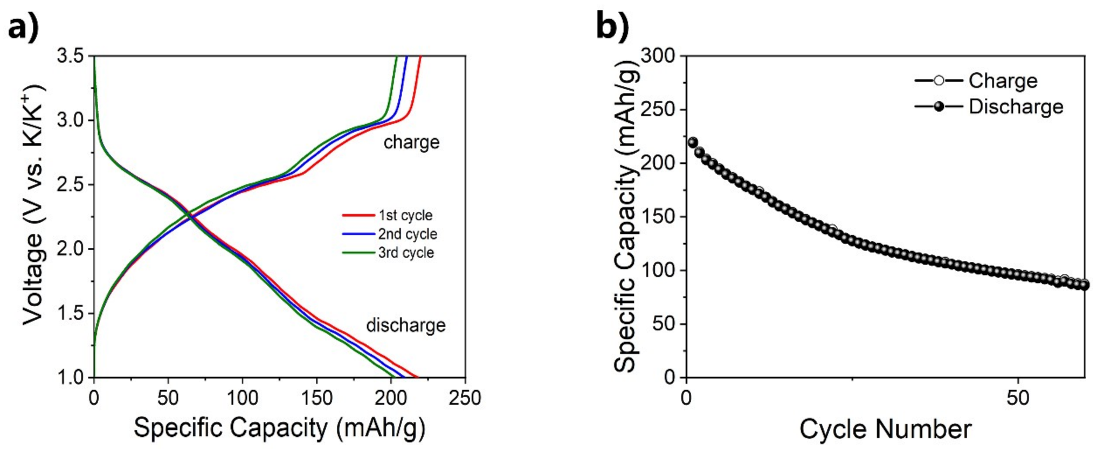

Figure S10. (a) GCD profiles at the first serveral cycles of the resultant fulle cell. (b) Cycling performance of the resultant fulle cell at 1 $A \cdot g^{-1}$ over 100 cycles.

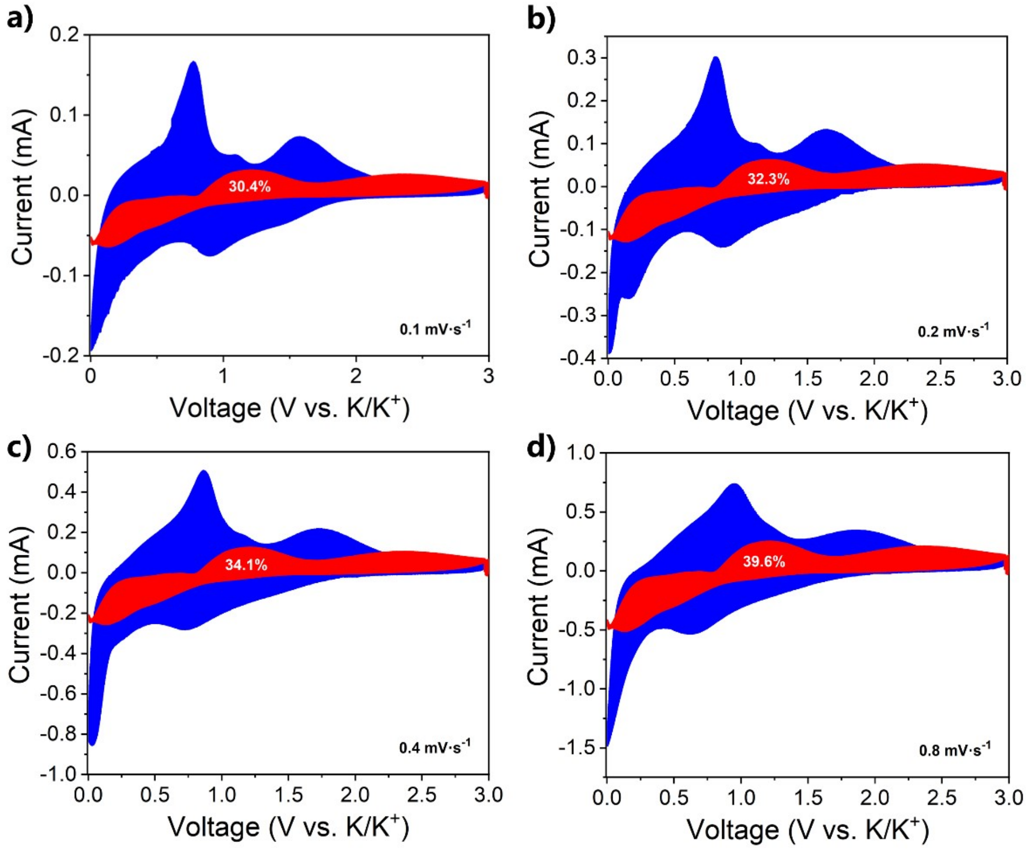

Figure S11. CV profiles of P@HPCN demonstrating the contribution of the surface-dependent process at scan rate of (a) 0.1 mV·s^{-1}, (b) 0.2 mV·s^{-1}, (c) 0.4 mV·s^{-1}, (d) 0.8 mV·s^{-1}.

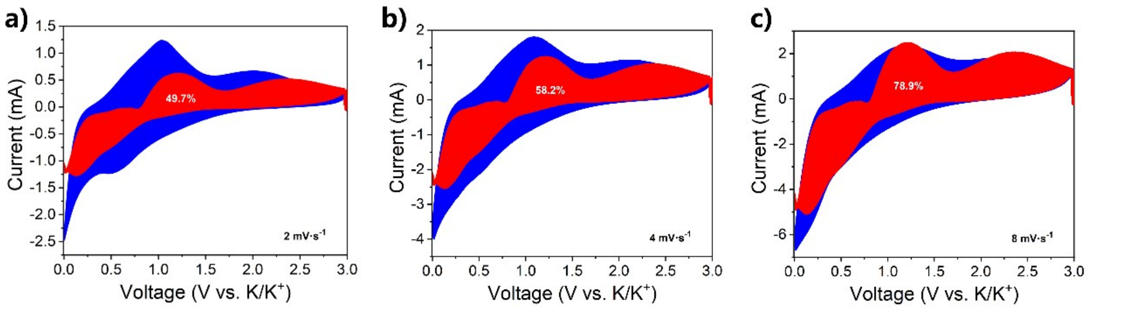

Figure S12. CV profiles of P@HPCN demonstrating the contribution of the surface-dependent process at scan rate of (a) 2 mV·s^{-1}, (b) 4 mV·s^{-1}, (c) 8 mV·s^{-1}.

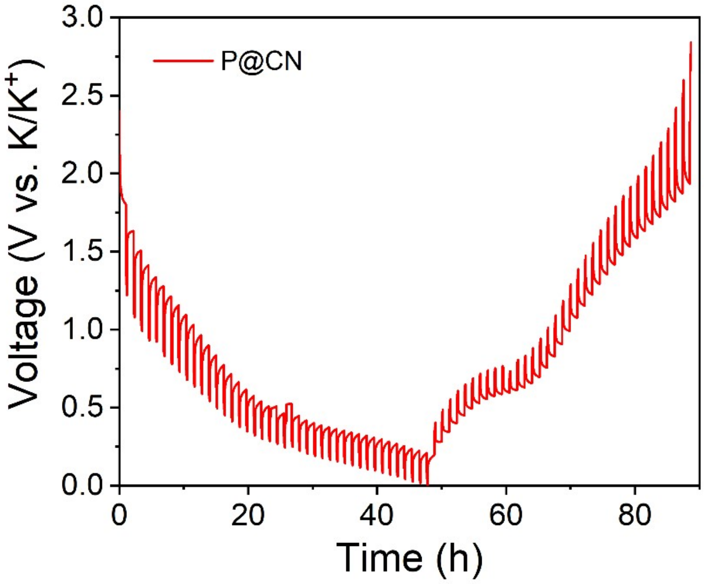

Figure S13. GITT profiles of the discharging and charging processes of P@CN.

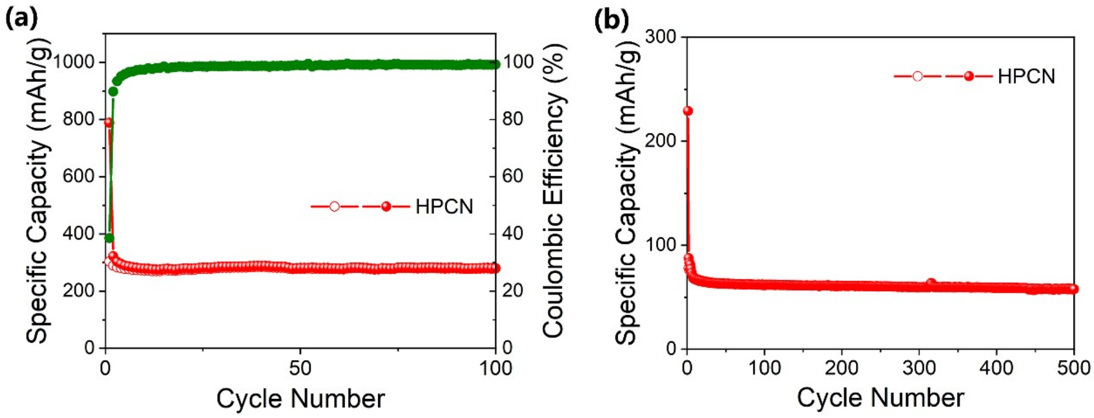

Figure S14. Cycling performance of HPCN at (a) 100 mA/g and (b) 1000 mA/g.

Table S1. Structure properties and surface chemistry of P@CN and P@HPCN

	I_G/I_D	at.% of total N 1s		
		Pyridinic-N	Pyrrolic-N	Graphitic-N
P@CN	1.10	18.07	55.55	26.38

P@HPCN	1.18	13.31	—	86.69

Table S2. Structure properties and surface chemistry of CN and HPCN

	S_{BET}(m2/g)	V_{pore} (cc/g)	$V_{micropore}$ (cc/g)	Element content (wt.%)		
				C	N	H
CN	770	0.954	0.258	77.41	8.06	1.383
HPCN	1051	1.01	0.376	89.61	3.60	0.798

Table S3. Comparison of the initial Coulombic efficiency, specific capacity at low current and long-term cyclability at large current for recent reported red phosphorus PIB anodes materials.

Sample name	**Initial Comlombic efficiency**	**Specific capacity**	**Long-term cyclability**	**References**
P@HPCN	**70.7%(0.1 A/g)**	**461.8 mAh/g at 0.1 A/g after 100 cycles**	**155.7 mAh/g at 1 A/g after 2000 cycles**	**This work**
P@AC@PPy	58.9%(0.02 A/g)	220 mAh/g at 0.05 A/g after 200 cycles	——	Nano Energy, 2020, 69, 104451
P@TBMC-2.4	63.5%(0.05 A/g)	396 mAh/g at 0.05 A/g after 75 cycles	244 mAh/g at 0.5 A/g after 200 cycles	Nano Energy, 2018, 52, 1-10
P@CN	59%(0.1 A/g)	427.4 mAh/g at 0.1 A/g after 40 cycle	——	Small, 2018, 14, 1802140
P50@ZCRod-0.025	78.5%(0.05 A/g)	401.8 mAh/g at 0.1 A/g after 75 cycle	150.7 mAh/g at 2.5 A/g after 400 cycles	Nano Energy, 2021, 83, 105797
P-C-2	58.8%(0.2 A/g)	512 mAh/g at 0.2 A/g after 200 cycle	212 mAh/g at 3.2 A/g after 10000 cycles	Nano Energy, 2021, 83, 105772
P@RGO	52.6%(0.1 A/g)	366.6 mAh/g at 0.1 A/g after 50 cycle	253 mAh/g at 0.5 A/g after 500 cycles	Chem. Eur. J, 2018, 24, 13897-13902

red P@N-PHCNFs	35%(0.1 A/g)	650 mAh/g at 0.1 A/g after 100 cycle	282 mAh/g at 5 A/g after 800 cycles	Nano Lett, 2019, 19, 1351-1358